TOPIC REVIEW

Treatment induced necrosis versus recurrent/progressing brain tumor: going beyond the boundaries of conventional morphologic imaging

Rajan Jain · Jayant Narang · Pia M. Sundgren ·
David Hearshen · Sona Saksena · Jack P. Rock ·
Jorge Gutierrez · Tom Mikkelsen

Abstract Brain tumor patients undergo various combinations therapies, leading to very complex and confusing imaging appearances on follow up MR imaging and hence, differentiating recurrent or progressing tumors from treatment induced necrosis or effects has always been a challenge in neuro-oncologic imaging. This particular topic has become more relevant these days because of the advent of newer anti-angiogenic and anti-neoplastic chemotherapeutic agents as well as use of salvage radiation therapy. Various clinically available functional imaging modalities can provide additional physiologic and metabolic information about the tumors which could be useful in identifying viable tumor from treatment induced necrosis and hence, can guide treatment planning. In this review we will discuss various functional neuro-imaging modalities, their advantages and limitations and also their utility in treatment planning.

Keywords Treatment induced necrosis ·
Recurrent/progressing brain tumor · Imaging ·
Progression · Pseudo-progression

Introduction

Treatment induced necrosis (TIN) is often an undesirable but unavoidable effect, and to differentiate this from recurrent or progressing tumors (RPT) on morphologic imaging studies has always been a challenge. Recent advances in brain tumor treatment have led to aggressive management strategies with combinations of surgery, chemotherapy, and radiation therapy based on the location and the histologic type of tumor. Various forms of radiation therapy including stereotactic radiosurgery, high-dose external beam radiation, and brachytherapy have become important therapeutic adjuncts. Recent use of various cytotoxic and anti-angiogenic agents has also increased patient survival and has added to the complexity of imaging response and recurrence patterns seen in these patients. Many of these patients undergoing adjuvant or concurrent therapy regimens often show increase in size of the enhancing lesion and/or edema which could be misinterpreted as progression of the tumor, whereas in fact, some of these changes could be attributed to 'pseudo-progression' [1]. This pseudo-progression could be a combination of treatment-induced necrosis, post-ictal changes, post-operative infarcts, and increased vascular permeability due to tapering of steroid dose as well as due to tumor growth [2]. Similarly, patients undergoing anti-angiogenic treatment may show very quick and marked reduction in the

R. Jain · J. Narang · D. Hearshen · S. Saksena
Division of Neuroradiology, Department of Radiology,
Henry Ford Hospital, Detroit, MI, USA

R. Jain (✉)
Division of Neuroradiology, Department of Radiology,
Henry Ford Health System, 2799 West Grand Blvd, Detroit,
MI 48202, USA
e-mail: rajanj@rad.hfh.edu

P. M. Sundgren
Department of Radiology, University of Michigan Hospital,
Ann Arbor, MI, USA

J. P. Rock · T. Mikkelsen
Department of Neurosurgery, Henry Ford Hospital,
Detroit, MI, USA

J. Gutierrez
Department of Pathology, Henry Ford Hospital,
Detroit, MI, USA

enhancement of the tumor even though those changes may not simply reflect treatment effects as non-enhancing infiltrative tumor may continue to grow. This marked reduction in the enhancement has been loosely referred to as 'pseudo-response'.

Conventional morphologic imaging features are usually inadequate to differentiate RPT from TIN. In addition, the problem is confounded by the fact that there is often a mixture of viable tumor with necrosis. Hence, it becomes particularly important to utilize many of the functional imaging techniques available today to follow these patients after treatment in order to characterize them correctly, as management plans for patients with RPT might differ significantly compared to those with TIN. Failure to recognize 'pseudo-progression' may result in premature discontinuation of effective adjuvant therapy, whereas including patients with 'pseudo-response' may result in a falsely high response rate to a therapy. The purpose of this review is to discuss various functional imaging modalities/techniques that can provide information about various metabolic (MR spectroscopic imaging, PET imaging) and physiologic (DWI, perfusion imaging) aspects of tumors and to also discuss the limitations of each modality in differentiating RPT from TIN.

Pathophysiology of treatment induced necrosis (TIN)

Radiation induced injury in brain is known to potentially target two cell populations, glial cells and vascular endothelial cells [3]. Additional mechanisms implicated in radiation injury include alteration of fibrinolytic enzyme mechanisms, and immune mechanisms that can cause autoimmune vasculitis. Direct injury to oligodendrocytes and vascular endothelial cells independently leads to demyelination and necrosis. Vascular injury causes vessel wall necrosis, vascular ectasia, and vascular telangiectasias, which may result in increased permeability and vasogenic edema. However, progressive vascular changes lead to vessel wall thickening, hyalinization of vessel wall, fibrinoid necrosis with consequent thrombosis and infarction followed by coagulative necrosis of the perivascular parenchyma. Radiation can also have direct cytotoxic effect upon glial cells and their progenitors. Apoptosis of mature oligodendrocytes, the cells that produce myelin, may be responsible for the demyelination that probably underlies early-delayed leucoencephalopathy. Radiation also damages O-2A progenitor cells, the precursor of both oligodendrocytes and type II astrocytes. Such damage, in combination with vascular damage, may cause late radiation necrosis. These radiation effects are often confounded by adjuvant or concurrent chemotherapy.

Various cytotoxic and anti-angiogenic agents are currently used for brain tumors and can lead to necrosis probably more quickly and dramatically than radiation therapy alone, hence further complicating the imaging response patterns. Anti-angiogenic agents, especially those targeting vascular endothelial growth factor (VEGF) such as bevacizumab and the VEGF receptor (VEGFR) including tyrosine kinase inhibitors such as cediranib, lead to decreased microvascular density, vascular permeability, and most importantly, inhibiting tumor growth in the process [4–7]. However, when VEGF-mediated angiogenesis is blocked, glioma cells may co-opt existing cerebral vasculature as an alternative to angiogenesis [4]. In a murine model, treatment with VEGF receptor antibody DC101 promoted satellite tumor formation with invasion along cerebral blood vessels [5] and similar findings were seen in rat gliomas [8]. Similar findings showing alteration in recurrence patterns of high-grade gliomas treated with bevacizumab have been suggested by some of the recent human studies [9]. These studies have suggested more effective suppression of enhancing tumor as compared to non-enhancing infiltrative tumor growth and more distant spread. Histopathological confirmation of this in human studies has been very limited as neurosurgical procedure providing tissue after salvage therapy with anti-angiogenic agents is usually not indicated due to the poor patient prognosis, complications such as bleeding, and poor wound healing related to another surgical procedure. However, one recent study [10] where surgical specimens were obtained from the patients treated with bevacizumab showed a robust up regulation of smooth muscle actin, CD34, fascin, and D2-40, suggesting progression towards a more primitive phenotype. Distant tumor recurrence could be explained by tumor cell migration to areas with robust perfusion.
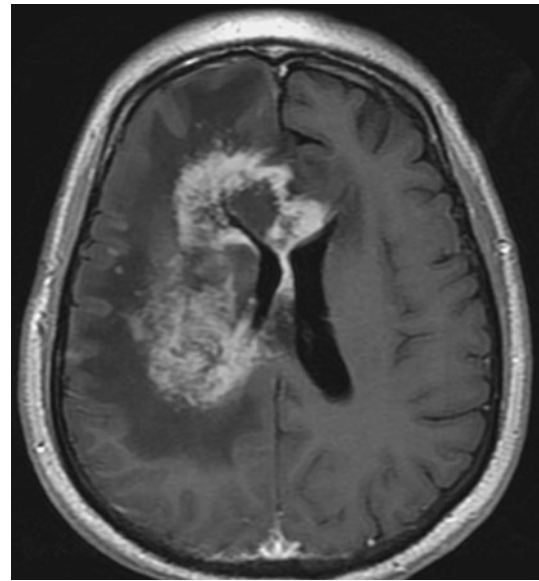
Morphologic MR imaging: limitations and pitfalls

Morphologic MR imaging characteristics of RPT include contrast enhancement, mass effect, and vasogenic edema. However, similar features are also seen with TIN/radiation necrosis and/or 'pseudo-progression' (Fig. 1). Kumar et al. [11] characterized radiation necrosis based on morphologic imaging features and showed that (1) conversion from no enhancement to enhancement, (2) remote new enhancement, (3) new periventricular enhancement, and (4) soap-bubble or swiss-cheese enhancement will favor radiation necrosis over recurrent and/or progressing tumor. Mullins et al. [12] demonstrated corpus callosum involvement, in conjunction with multiple enhancing lesions with or without crossing of the midline and sub-ependymal spread favor predominat glioma progression thus contradicting
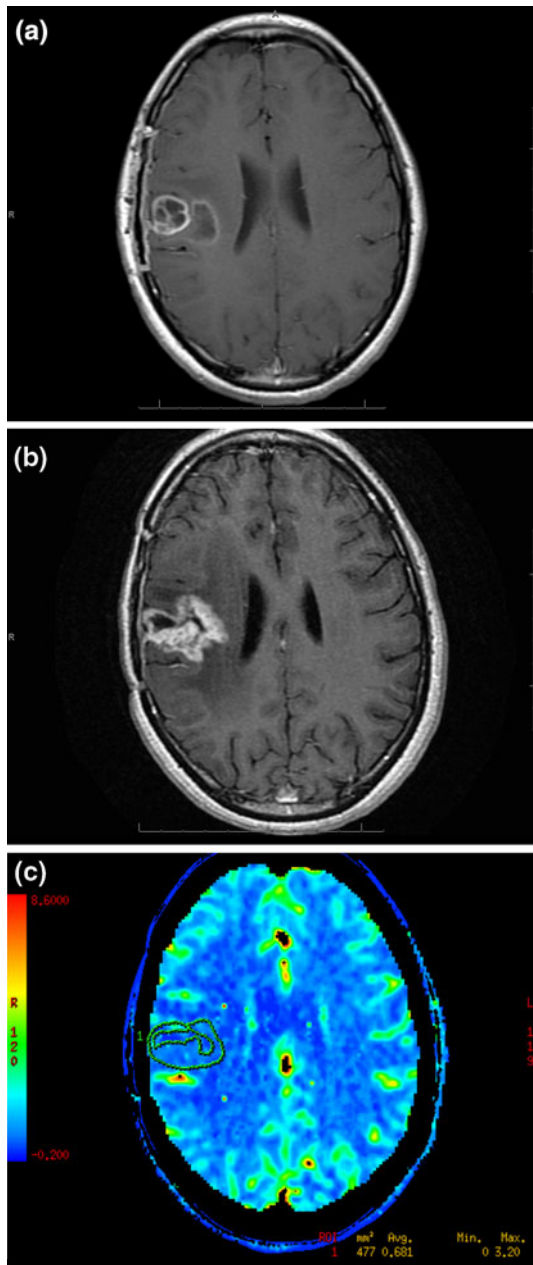
Fig. 1 37-years old female with a recurrent right fronto-parietal GBM was treated with radiation therapy showed progression in the contrast enhancing lesion from (a) baseline study to (b) 6 months follow up post-radiation therapy. CT perfusion study showed reduced (c) blood volume suggesting treatment effects or radiation necrosis which was proven with histopathology

Fig. 2 Histopathology proven radiation necrosis in a patient previously irradiated grade III glioma showing heterogeneously enhancing lesion with swiss-cheese pattern and ill-defined spreading wave front like margins involving the corpus callosum and periventricular regions
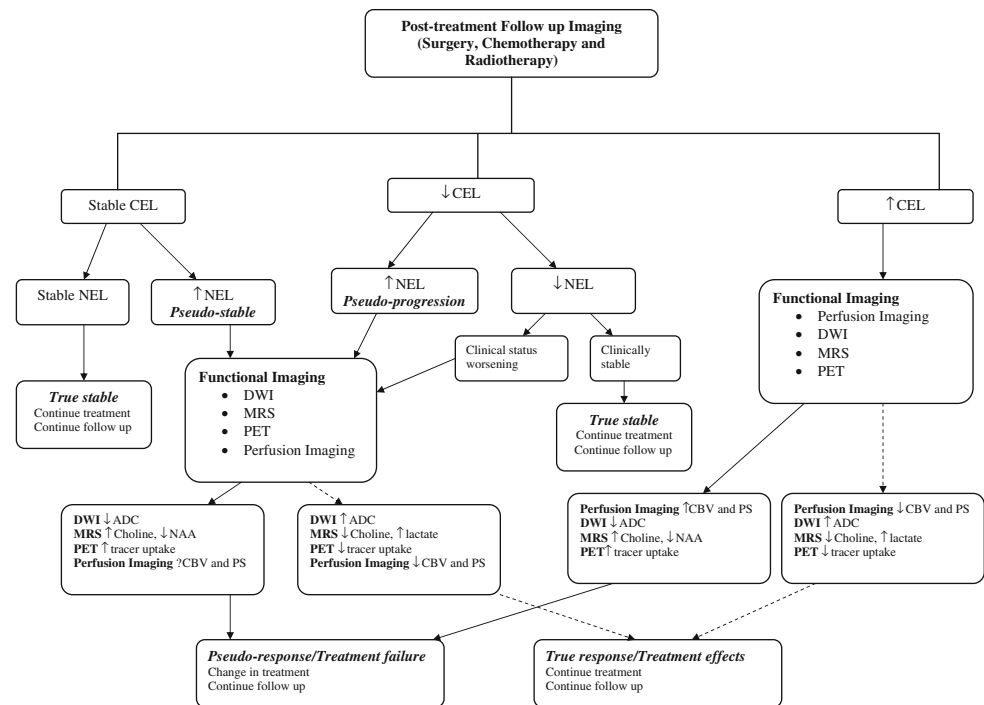
some of the previously described morphologic features described by Kumar et al. [11]. Mullins et al. [12] also stressed that combinations of enhancement patterns were more likely than individual patterns to distinguish necrosis from tumor progression. In our experience, we have noted a high percentage of cases with histopathology proven radiation necrosis showed periventricular/sub-ependymal spread (50%) and corpus callosum involvement (27%)

(Fig. 2), hence, suggesting that dependence on only morphologic imaging features could be misleading [13]. Similarly, with the increasing use of anti-angiogenic agents, the utility of only contrast enhancement as a feature of tumor recurrence has also been questioned. Non-enhancing infiltrative tumor recurrence or progression, which could occur at or away from the primary tumor site in these patients, has further unmasked the limitation of using only contrast enhancement or conventional morphologic features as the criteria for assessing treatment response [6, 9, 14, 15]. Because of the limitations of using only morphologic imaging features such as RECIST (Response Evaluation Criteria in Solid Tumors) or Macdonald criteria as a measure of treatment response, there has also been an international effort in neuro-oncology to improve imaging response assessments for high-grade gliomas by adding information about a patient's clinical status to various morphologic imaging features, and to especially allow the interpretation of clinical trials involving anti-angiogenic agents (Response assessment in neuro-oncology working group, RANO). However, none of these criteria include any functional imaging techniques as a treatment response measure primarily because of lack of standardization of image acquisition, post-processing, and image analysis. Many of these functional imaging techniques, whether evaluating tumor physiology (DWI and perfusion imaging) or assessing tumor metabolism (MR spectroscopy, PET based imaging techniques), have been used alone or in various combinations to differentiate RPT from TIN [16–

Fig. 3 Post treatment follow up imaging algorithm

Post-treatment Follow up Imaging (Surgery, Chemotherapy and Radiotherapy)

- Stable CEL
  - Stable NEL
    - **True stable** — Continue treatment, Continue follow up
  - ↑NEL **Pseudo-stable**
    - **Functional Imaging**
      - DWI
      - MRS
      - PET
      - Perfusion Imaging
- ↓CEL
  - ↑NEL **Pseudo-progression**
  - ↓NEL
    - Clinical status worsening
    - Clinically stable
      - **True stable** — Continue treatment, Continue follow up
- ↑CEL
  - **Functional Imaging**
    - Perfusion Imaging
    - DWI
    - MRS
    - PET

DWI ↓ADC
MRS ↑Choline, ↓NAA
PET ↑tracer uptake
Perfusion Imaging ?CBV and PS

DWI ↑ADC
MRS ↓Choline, ↑lactate
PET ↓tracer uptake
Perfusion Imaging ↓CBV and PS

Perfusion Imaging ↑CBV and PS
DWI ↓ADC
MRS ↑Choline, ↓NAA
PET ↑tracer uptake

Perfusion Imaging ↓CBV and PS
DWI ↑ADC
MRS ↓Choline, ↑lactate
PET ↓tracer uptake

Pseudo-response/Treatment failure — Change in treatment, Continue follow up

True response/Treatment effects — Continue treatment, Continue follow up

20]. We propose following a flexible algorithm in post-treatment patients, starting with conventional morphologic imaging features using standard of care follow up MR imaging and incorporating some of these functional imaging tools as needed (Fig. 3).

Dynamic contrast enhanced imaging: perfusion imaging techniques

Dynamic contrast-enhanced imaging techniques using MRI or CT have been used to obtain measures of tumor vascular physiology and hemodynamics. Many of the perfusion parameters have been correlated with tumor grade, aggressiveness, and prognosis [21–24]. Regional tumor blood volume measurements reflect an assessment of tumor vasculature and perfusion, and have been correlated with glioma grading as well as prognosis. Hypoxia or hypoglycemia, occurring in rapidly growing tumors, increases the expression of vascular endothelial growth factor (VEGF) which is not only a potent angiogenic factor, but also a potent permeability factor [7, 25]. VEGF leads to the development of neoangiogenic vessels which are immature, tortuous [26], and also have increased permeability to macromolecules. These abnormal tumor vessels and their hemodynamic parameters can be used as potential markers to detect RPT in previously treated patients.

Neo-angiogenesis and high density of tumor vessels usually shows as regions of hyper perfusion and increased blood volume. Chronic radiation injury causes vascular endothelial damage and progressive vascular changes like vessel wall thickening caused by hyalinization with consequent thrombosis, infarction, and coagulative necrosis [27]. Radiation necrosis thus primarily consists of ischemic changes caused by occlusive vasculopathy, leading to infarction and regions of hypoperfusion showing reduced blood volume. However, tumor vasculature and perfusion also depends on a number of other variables and is usually very heterogeneous. In a rapidly growing, high grade tumor, tumor vasculature can be severely compromised due to the rapid growth of the tumor cells, necrosis, and increased permeability of the vessels causing interstitial edema, which can also cause compression of the smaller vessels leading to areas of hypoperfusion. MR perfusion has particularly been used for evaluation of hemodynamic characteristics of brain tumors [28], and has also been used for differentiating recurrent tumor from radiation necrosis successfully [29]. In one study, the authors concluded that rCBV (relative cerebral blood volume) ratio >2.6 suggest tumor recurrence and a ratio <0.6 may suggest non-neoplastic contrast enhancing lesion. However, they also suggested that when the ratio is between 0.6 and 2.6, ^{201}Tl SPECT might be useful in differentiation of recurrent tumor from radiation necrosis [30].

Disadvantages of MR perfusion include limited availability and more complex quantification of various perfusion parameters because of a nonlinear relationship between tissue signal intensity and contrast agent concentration as well as difficulty in assessing an arterial input function as compared to perfusion CT. Perfusion CT is
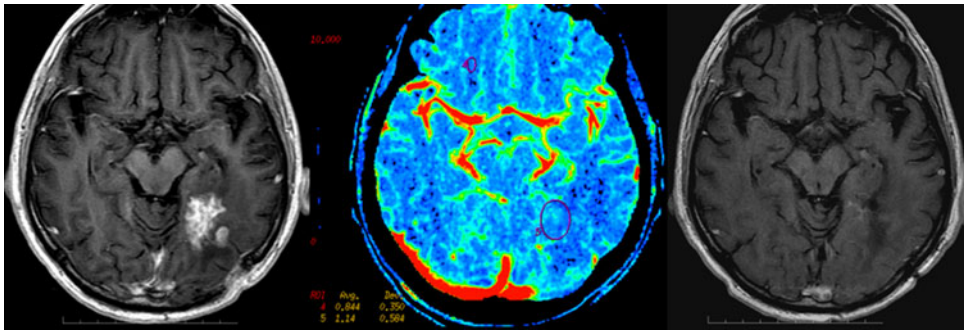
Fig. 4 50 years old male previously treated with SRS (stereotactic radiosurgery) for cerebral metastasis from lung cancer. Post contrast T1-weighted axial images showing a recurrent heterogenously enhancing lesion in the left temporo-occipital region. Perfusion CT blood volume map showing decreased blood volume consistent with a diagnosis of radiation necrosis. Six months follow up post contrast T1-weighted axial images (extreme right) showing resolution of the enhancing lesion without any anti-neoplastic treatment

more readily available and has been recently employed for assessment of brain tumors [24, 27], as well as differentiating radiation necrosis from recurrent tumors with very good success [31], and probably also has the advantage of having very robust data (Figs. 1c, 4). Use of an arterial input and a venous output function helps to generate quantitative perfusion parametric maps. Jain et al. reported a cutoff point of 1.65 for nCBV (normalized CBV) with a sensitivity of 83.3% and specificity of 100% to diagnose recurrent tumor from radiation necrosis using perfusion CT [31]. However, radiation exposure and use of an iodinated contrast agent limit the utility of perfusion CT in brain tumor assessment where as MR perfusion can be obtained as an additional sequence to standard of care contrast enhanced MRI done for these patients.

Perfusion assessment of post-treatment patients is usually complicated by the fact that many of these patients have a mixture of tumor recurrence and radiation necrosis. Recurrent tumors may not always consist of only tumor cells but probably also contain tumor necrosis as well as hypovascular areas caused by radiation-induced occlusive vasculopathy, thus reducing CBV in mixed tumor necrosis as compared to predominant high-grade tumors. Depending upon how much necrosis and tumor cell density a lesion has, perfusion parameters such as CBV can show lower values. Similarly, within irradiated brain tissue, in addition to occlusive vasculopathy, a variety of other vascular phenomena are noted, such as aneurysmal formation, telangiectasia, vascular elongation, and a remarkable proliferation of endothelial cells, especially in the capillary bed [32] which can even increase CBV in radiation necrosis and therefore inducing some overlap of the perfusion parameters. Perfusion imaging could also have a limited role, especially in patients who are on anti-angiogenic agents and show 'pseudo-response' because of the 'vascular normalization' effect of these agents [16, 33], even though infiltrative tumor might continue to grow. In such a scenario, other physiologic measures not completely based on tumor perfusion such as DWI [9], metabolic measures such as MR spectroscopy, or PET imaging might be more helpful in differentiating TIN from RPT.

Tumor vessel permeability estimates, another important aspect of tumor physiology that has not been explored much particularly to differentiate RPT from TIN, can also be assessed using MR or CT perfusion techniques. Kamiryo et al. [34] have also demonstrated that blood–brain-barrier architecture of capillaries within previously irradiated brain tissue remains intact despite a decrease in the mean capillary density as well as increased capillary diameter, thus suggesting that permeability measurements may also help differentiate radiation necrosis from recurrent tumors. Barajas et al. [29] recently demonstrated significantly lower percentage signal intensity recovery in radiation necrosis as compared to recurrent metastatic intra-axial tumors using DSC T2* MR perfusion, however, also noting major limitation of susceptibility artifacts resulting in image degradation making DSC measurements difficult to obtain. DCE T1-weighted MR perfusion techniques which are not affected by susceptibility artifacts can help obtain a better estimation of vascular leakiness and can show lower K_{trans} measurements in TIN as compared to RPT (Fig. 5).

Proton magnetic resonance spectroscopy (^{1}H-MRS)

Proton magnetic resonance spectroscopic imaging has been particularly promising given the heterogeneity of these lesions. Data can be obtained using single-voxel or multi-voxel techniques with either 2D or 3D CSI (chemical shift imaging) sequences. Comparing multi-voxel MRS with single-voxel MRS and FDG-PET, Chong et al. [35] showed a sensitivity and specificity of 100% for multi-voxel MRS as compared to 50% sensitivity for both single-voxel MRS and FDG-PET. However, there are technical challenges and despite having good success in multiple
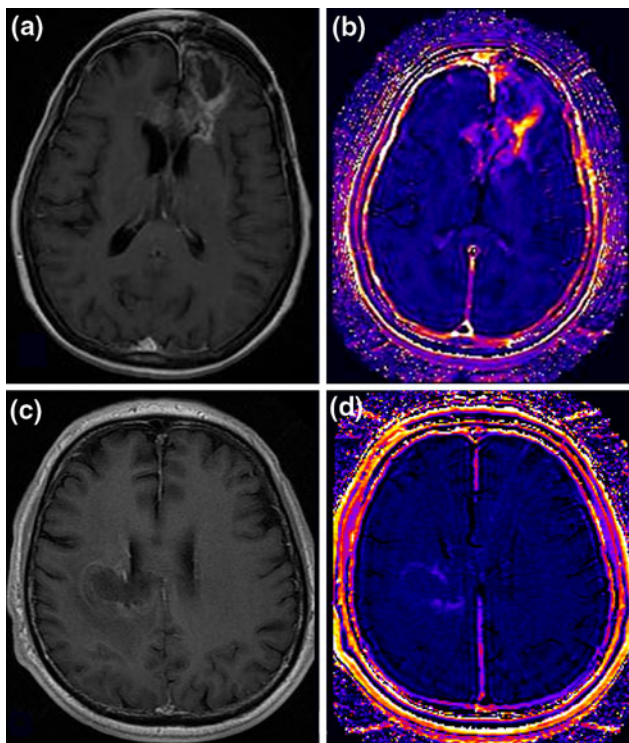
Fig. 5 *a* Post-contrast T1-weighted axial image in a patient with left frontal recurrent enhancing lesion showing (*b*) higher vascular leakiness on DCE T1-MR perfusion K_{trans} maps suggesting recurrent/progressive tumor. *c* Another patient with recurrent enhancing lesion in right frontoparietal region showed (*d*) lower permeability on DCE T1-MR perfusion K_{trans} maps suggesting radiation necrosis which was confirmed with stereotactic biopsy and histopathology from the enhancing part

studies [36–38], MRS has also shown some limitations, particularly due to its limited spatial resolution. Recently, improvements in spatial resolution and chemical specificity available at 3 Tesla have increased the ability of MRS to differentiate recurrent tumor from radiation effects [39].

Spectral patterns in radiation necrosis have been shown to have decreased NAA and variable changes in Cho and Cr [17, 35, 38–42]. Increases in Cho have been observed in normal appearing contralateral white matter within the first few months after radiation [43, 44], while significant decreases in Cho relative to pretreatment levels have been observed in later stages of radiation necrosis [38]. In addition, radiation necrosis may also show a broad peak corresponding to cellular debris containing fatty acids, lactate (Lac), and amino acids [45]. Weybright et al. [36] reported a cutoff value of >1.8 for either Cho/NAA or Cho/Cr for diagnosis of tumor recurrence, but there were cases classified as tumor recurrence that did not have a voxel with Cho/NAA or Cho/Cr >1.8. In these patients the NAA/Cr ratios were elevated compared to the group with Cho/NAA >1.8, consistent with partial volume contamination of non tumor tissue in the measured voxels. Smith et al.

[37] suggested a prediction model for probability of recurrent tumors using Cho/NAA ratio with sensitivity of 85% and specificity of <70%. Many of these studies have the major drawback of having limited correlation with histopathology. Rock et al. [38] compared MRS measures directly with histopathology of image guided biopsy specimens where the biopsy and MRS voxel locations were registered to the same coordinate system. Their results suggested that metabolite ratios allow reliable differentiation between pure tumor and pure necrosis, but the spectral patterns were less definitive when tissues composed of varying degree of mixed tumor and necrosis. These authors demonstrated a sevenfold-increased odds of being pure tumor compared with pure necrosis with a Cho/Cr ratio of >1.79 or lipid (lip) and lactate/Cho ratio of <0.75 in all histopathology proven image-guided specimens. These three studies demonstrate the limitations of current methodology. Where MRS samples pure tissue it can reliably differentiate recurrent tumor from radiation necrosis, for example, with Cho/Cr or Cho/NAA >1.79, but where there are heterogeneities below the current spatial resolution limits, ~ 1 cc, admixtures of normal brain, recurrent tumor, and/or radiation necrosis cannot be reliably characterized. Despite this limitation, MRS can provide valuable information in the assessment of recurrent tumor (Fig. 6) versus radiation necrosis (Fig. 7), particularly in conjunction with other imaging and clinical data. The timing of MRS measurements relative to treatment must be taken into consideration, given potential increase in Cho/Cr in apparently normal brain tissue in the short term (Fig. 8). Longer scan times required to obtain reproducible data is another hindrance to the widespread use of MRS. However, parallel imaging strategies may allow an increase in spatial resolution in conjunction with decreases in examination time and should increase the utility of MRS for this application.

Diffusion weighted and diffusion tensor imaging

Diffusion weighted imaging (DWI) is sensitive to microscopic displacement of water molecules which is impeded by the presence of structures on the cellular scale. DWI has been used in the assessment of tumor cellularity and treatment response [46–52]. A more complex and complete form of diffusion imaging, diffusion tensor imaging (DTI) has, for example, been able to demonstrate white matter tract altered by tumor [53], information that can be valuable in pre-surgical planning, differentiating high-grade gliomas, and to evaluate the extent of cellular infiltration [19, 54]. In DTI, the directionality of water is probed by application of diffusion-sensitization gradients in multiple directions [55]. Studies using more sophisticated methods
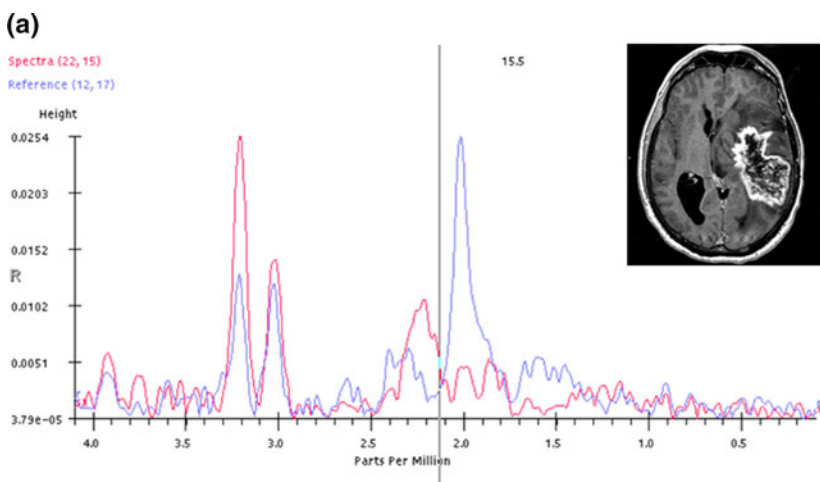
Fig. 6 Postcontrast T1-weighted MR image (*inset*) showing a recurrent enhancing lesion in a patient with previously treated high grade glioma. MR spectroscopy from the lesion (*blue*) showing increased Cho (*arrow*) with decrease in the NAA suggestive of recurrent tumor. Spectrum from the contralateral normal appearing white matter showing normal levels of the metabolites (*red*). Corresponding metabolite maps are also shown
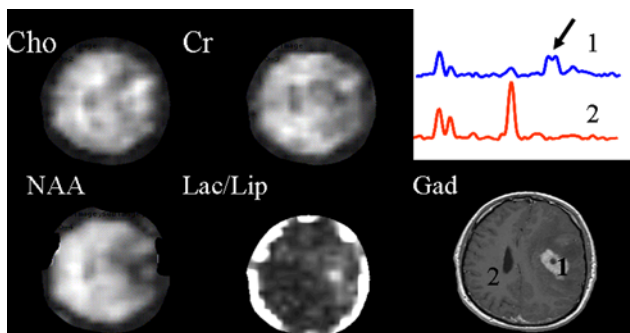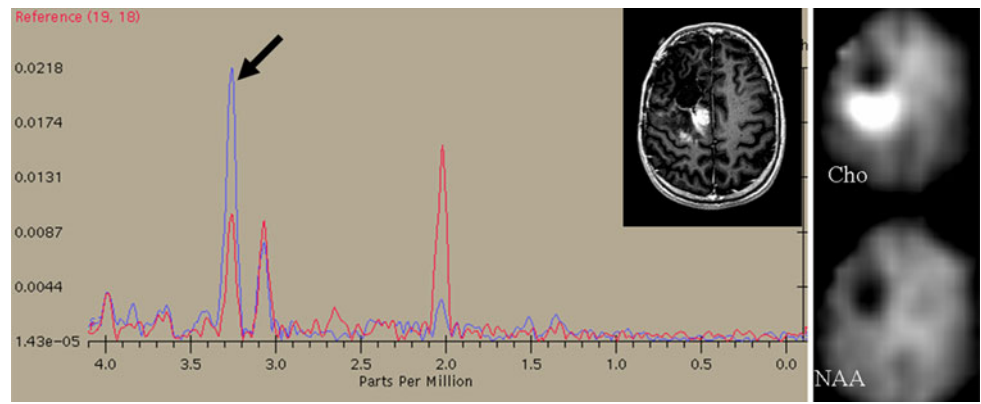

Fig. 7 Bottom right, T1-weighted post contrast image showing the location of recurrent enhancing lesion (1) and normal-appearing white matter (2) used for reference. Top right, spectrum from the voxel corresponding to the biopsy (1) showing reduced levels of Cho, Cr and NAA and a Lac/Lip peak (*arrow*) suggestive of radiation necrosis. Spectrum from the normal appearing white matter (2) showing normal levels of Cho, Cr and NAA and absence of Lac/Lip. The corresponding metabolite maps are also shown (*extreme left*)

for evaluation of tumors, such as analysis of the role of the different eigenvectors, have demonstrated that the value of the major eigenvector of the diffusion reflecting the diffusivity in the longitudinal direction was significantly lower in white matter surrounding glioma than in white matter surrounding metastases even when the anisotropy showed no difference [56].

There is some disagreement in the literature regarding which lesion type, recurrent tumor or radiation necrosis, has higher ADC values [18, 57–61]. In a previous study evaluating new contrast enhancing lesions in patients previously treated for brain neoplasm, the authors utilized quantitative values of ADC, FA, and the Eigen values and ratios derived from the diffusion tensor in the white matter tracks in and surrounding the lesion [57]. That study found significantly higher ADC values in the contrast-enhancing lesion in patients with recurrent tumor compared to those

Fig. 8 a Postcontrast T1-weighted MR image (*inset*) showing a recurrent enhancing lesion in a patient with previously treated high grade glioma. MR spectroscopy from the enhancing lesion (*red*) showing increased Cho/Cr with decrease in the NAA suggestive of recurrent tumor. Spectrum from the contralateral normal appearing white matter showing normal levels of the metabolites (*blue*).
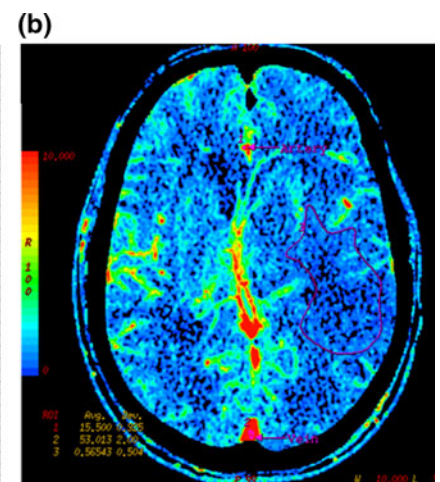
b However, perfusion CT blood volume map showed reduced blood volume in the lesion suggesting predominant treatment effects. Histopathology revealed pure radiation necrosis with no viable tumor cells confirming that Cho/Cr ratio was probably increased due to active demyelination rather than due to tumor

values seen in patients with radiation injury. They also found both $\lambda_{\parallel}$ (prinicipal eigenvalue parallel to the predominant orientation of axonal fibers, axial diffusivity) and $\lambda_{\perp}$ values (mean of second and third eigenvalues perpendicular to axonal fibers, radial diffusivity) to be significantly higher in the contrast enhancing lesion in patients with recurrent tumor compared to those with radiation injury. In contradiction to these findings a previous study found both ADC and ADC ratios to be significantly lower in the recurrent group compared to non-recurrent group [18]. Similar findings with the maximal ADC values being significantly smaller for recurrent tumor than for radiation necrosis was also seen in recent study by Asao [62]. The addition of ADC values to the metabolic ratios NAA/Cho and NAA/normal Cr seems to have added value as it increases the odds of correct differentiation between pure tumor and pure radiation necrosis [38].

The relationship between the FA value and different histological types and grade of astrocytic tumors has previously been reported [19, 63], and also changes in FA values due to radiation induced effect on normal white matter in patients with cerebral gliomas [64], but few reports on use of FA values to differentiate recurrent tumors from radiation injury exists. In a recent case report of three cases of new enhancement after radiotherapy lower FA values was found in the enhancing portion of the lesion in the case of radiation necrosis than the values found in the two cases of recurrent tumor [65]. Sundgren et al. [57] did not find any differences in the FA values between recurrent tumors and radiation necrosis when evaluating the contrast enhancing portions of 28 lesions, however they found the FA ratio to be significantly higher in normal appearing white matter adjacent to the peri-lesional edema in patients diagnosed with radiation necrosis compared to those found in patients with recurrent tumor.

PET based techniques

Assessment of the metabolic state of the recurrent enhancing lesion has been done to differentiate RPT from radiation necrosis using FDG-PET, ^{11}C-methionine PET, other amino acid analogue tracers, and ^{201}Tl SPECT with mixed success [66–68]. Use of PET is based on the fact that RPT will show increased metabolism due to active tumor cells whereas TIN will show low metabolism and tracer uptake (Fig. 9). Such observations were first reported by Patronas et al. [69] in 1982. However, very high and variable FDG uptake by normal cortex makes it difficult to distinguish tumors from adjacent normal gray matter, especially when no significant edema surrounds the lesion. In addition, low-grade gliomas usually appear as hypometabolic when compared with normal cortex [70],

limiting the potential of FDG-PET for detecting such progressing lesions. Various non-neoplastic diseases that also display increased glucose metabolism are potential sources of false-positive results. For instance, brain abscesses can show increased FDG uptake [20]. Radiation injury can activate repair mechanisms or lead to inflammatory activity, which can increase glucose metabolism and result in false positive results. Limited availability and low spatial resolution are some of the other limitations of PET and SPECT scanning. FDG-PET showed a sensitivity of 75% and specificity of 81% to diagnose recurrent tumor [66] whereas another study comparing ^{201}Tl SPECT with FDG-PET showed a higher sensitivity of 92% with ^{201}Tl SPECT as compared to 62% with FGD-PET [67].

Amino acid and amino acid analog PET tracers are currently being used in brain tumor imaging. Amino acid imaging is based on the observation that amino acid transport is generally increased in malignant transformation. ^{11}C-methionine PET has been widely used for glioma grading, differentiation of neoplastic from non-neoplastic lesions and radiation necrosis from tumor recurrence (Fig. 10) [20, 71]. One study showed 100% sensitivity, 60% specificity, and 82% overall accuracy in the detection of tumor recurrence with ^{11}C-methionine PET [71]. To a large extent, the intensity of ^{11}C-methionine uptake is related to the grade of the tumor but the uptake by the normal cortex is low, and most low-grade tumors are easily detected.

Recently, several reports have been published that show the potential clinical utility of a new compound in brain tumor imaging 18F-FLT-PET (3_-deoxy-3_-[18F]fluorothymidine) [72, 73] 18F-FLT is not taken up in normal brain cells due to essentially no proliferative activity and an intact blood brain barrier. This gives it a distinct advantage compared with FDG, as it will only be concentrated in a proliferating tumor and thus allows for improved differentiation of necrosis from recurrence and differentiation of low- and high-grade brain tumors. Another agent in this group that has been used with success is ^{18}F 3,4-dihydroxy-6-18F-fluoro-L-phenylalanine (^{18}F-FDOPA) [74], however limited availability is a major limitation.

Usually new or recurrent enhancing lesions on MR imaging that show increased FDG uptake, equal to or greater than that in normal cortex, are likely to represent tumor recurrence. Sensitivity is an issue with FDG PET, especially with low-grade gliomas. However with less false-positive results, specificity is usually high in routine clinical practice. A combination of FDG with a radiolabeled amino acid analogue like ^{11}C-methionine or newer compounds can provide a comprehensive characterization of suspected brain tumor recurrence. Co-registration with MR imaging will surely improve the diagnostic performance of FDG-PET because it helps delineate the

Fig. 9 Post-contrast T1-weighted MR images showing a recurrent enhancing lesion in a patient with previously treated tumor. FDG-PET scan done shows reduced tracer uptake (*arrow*) suggestive of hypometabolism and histopathology revealed radiation necrosis
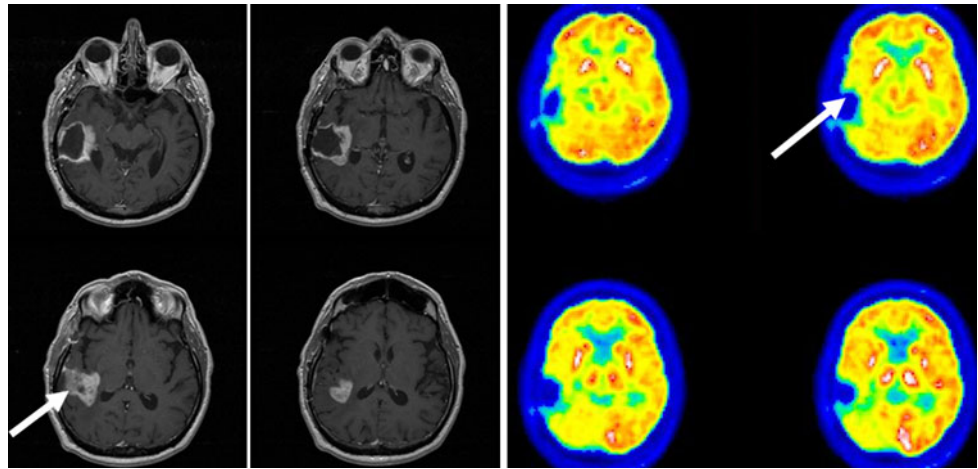
Fig. 10 ^{11}C-methionine PET study done in a patient with recurrent contrast enhancing lesion (*inset*), shows increased tracer uptake consistent with a diagnosis of recurrent tumor (*arrows*)
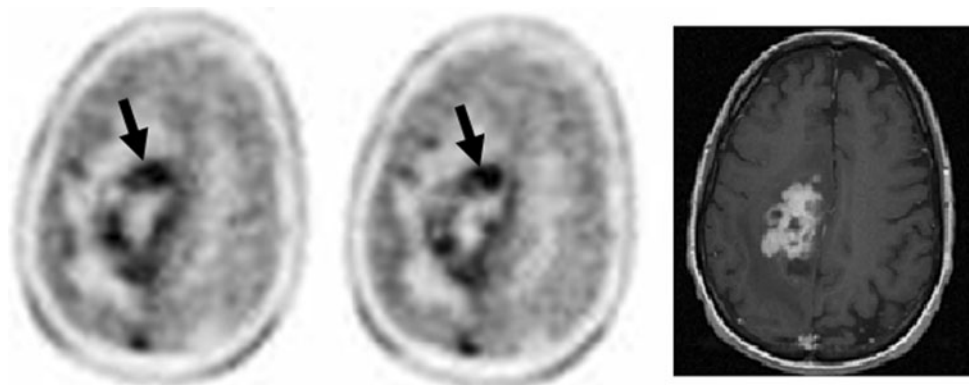
suspicious area and any increased uptake in the suspicious or enhancing abnormality on MRI can be considered as RPT.

Utility of functional imaging for monitoring treatment response and for targeting treatment and/or biopsy

One of the major hurdles in using any of these functional imaging techniques as a follow up tool to quantify treatment response is lack of standardization of image acquisition and post-processing for most of the techniques. Many of these measures can vary depending upon the scanner type and strength used (particularly true for ADC and eigenvalues) [75], type and strength of the tracer/contrast agent and bolus used apart from change in patient's hemodynamics on follow up visits. Many of these factors significantly limit absolute quantification of these physiologic and metabolic measures. This has been compensated to some degree by using relative values obtained by dividing absolute values from the lesion with absolute values obtained from the normal appearing white or gray matter. Because of these, there is also lack of development of standard values for many of these functional parameters

and hence, these measures cannot be implemented across multiple centers. However, recently dynamic contrast enhanced MR imaging has been used to estimate vascular permeability in recurrent glioblastomas treated with cediranib to assess treatment response [76]. Water diffusivity measurements have also been used to assess treatment response and tumor growth patterns in the recent past [9, 77–79]. Most of the discussed functional imaging techniques can potentially be useful for targeting foci of tumor in a heterogeneous mixture of tumor and necrosis for biopsy and radiation planning. Foci of tumor which appear as 'hot spots' i.e. usually show high metabolism or perfusion, due to active, mitotic tumor cells in a heterogeneous mixed tumor necrosis lesion may be targeted to increase the yield of a surgical biopsy procedure. Similarly, targeted radiation therapy with a boost to the 'hot spots' potentially can increase the effectiveness while limiting neurotoxicity in the future (Fig. 11).

Conclusions

In conclusion, even though many of these non-invasive functional imaging techniques can help evaluate post-

Fig. 11 59 year old male, previously treated for a malignant glioma with chemotherapy and radiation, developed radiation necrosis proven with histopathology and remained stable for 4 years. **a** Follow up imaging showed recurrent enhancing lesion (*arrowheads*) in the previously stable heterogeneously enhancing radiation necrosis (*arrows*). DCE T1-MR perfusion parametric maps showed increased (**b**, **c**) blood volume and (**d**, **e**) K_{trans} in the recurrent enhancing lesions (*arrowheads*) as 'hot spots' suggesting recurrent tumor, with in relatively low blood volume and K_{trans} stable radiation necrosis region (*arrows*). These 'hot spots' were used for the planning of fractionated re-irradiation. **f** Radiation therapy isodose lines showing higher dose delivered to the hot spots with relative sparing of the previously stable radiation necrosis region
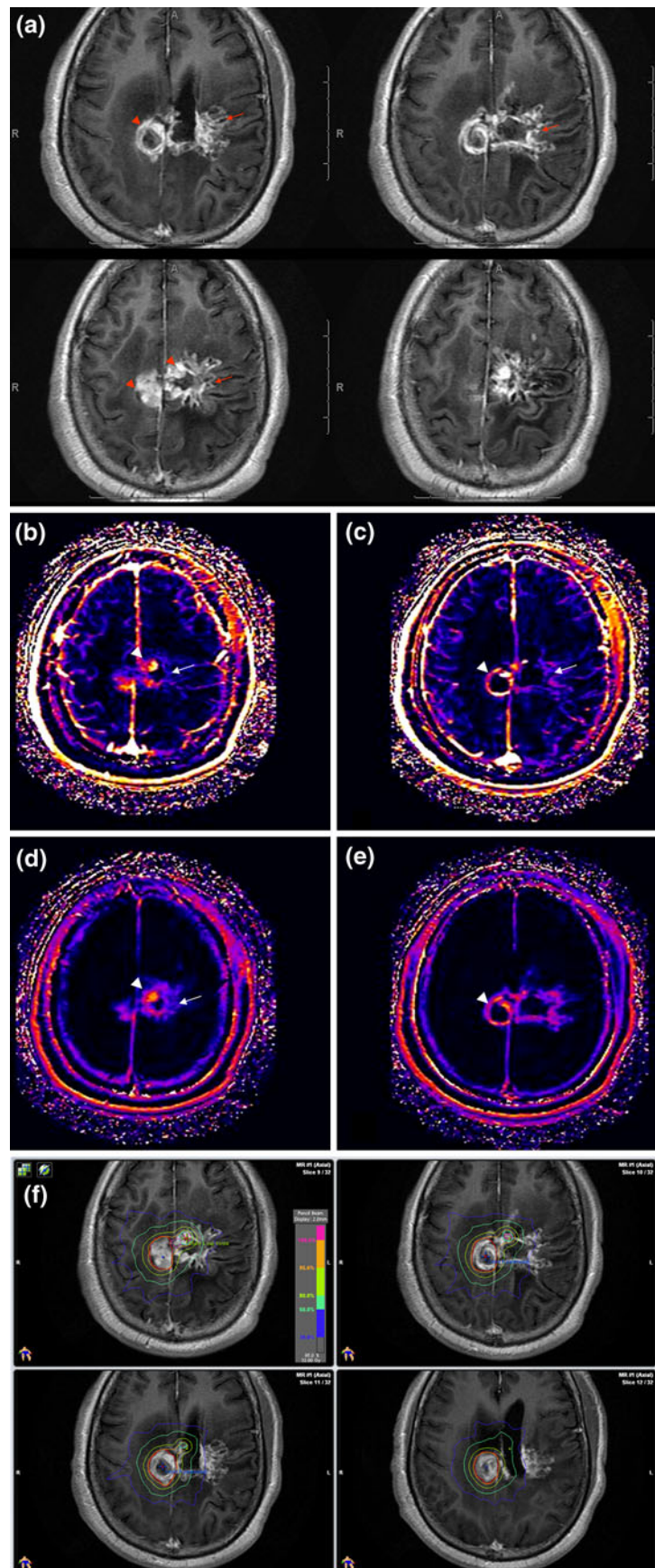
treatment patients following various combination therapies, there is lack of standardization as far as image acquisition and post-processing is concerned across multiple centers. Another major limitation with most of these techniques is limited resolution which is further complicated by the fact that most of the patients after treatment have mixture of RPT and TIN in varying degrees, therefore making in vivo quantitative assessments extremely difficult. Despite these limitations, there is a greater need to develop and use some of these functional imaging biomarkers as with the advent of newer chemotherapeutic agents and use of combination therapies, recurrence patterns and adverse treatment effects seen on conventional imaging have become too complex. Functional imaging modalities can also be used for treatment guidance once RPT and TIN could be differentiated in vivo in a mixture of heterogeneous appearance seen on morphologic imaging.

References

1. Chamberlain MC, Glantz MJ, Chalmers L, Van Horn A, Sloan AE (2007) Early necrosis following concurrent Temodar and radiotherapy in patients with glioblastoma. J Neurooncol 82:81–83
2. Clarke JL, Chang S (2009) Pseudoprogression and pseudoresponse: challenges in brain tumor imaging. Curr Neurol Neurosci Rep 9:241–246
3. Lyubimova N, Hopewell JW (2004) Experimental evidence to support the hypothesis that damage to vascular endothelium plays the primary role in the development of late radiation-induced CNS injury. Br J Radiol 77:488–492
4. Holash J, Maisonpierre PC, Compton D, Boland P, Alexander CR, Zagzag D, Yancopoulos GD, Wiegand SJ (1999) Vessel cooption, regression, and growth in tumors mediated by angiopoietins and VEGF. Science 284:1994–1998
5. Kunkel P, Ulbricht U, Bohlen P, Brockmann MA, Fillbrandt R, Stavrou D, Westphal M, Lamszus K (2001) Inhibition of glioma angiogenesis and growth in vivo by systemic treatment with a monoclonal antibody against vascular endothelial growth factor receptor-2. Cancer Res 61:6624–6628
6. Sorensen AG, Batchelor TT, Wen PY, Zhang WT, Jain RK (2008) Response criteria for glioma. Nat Clin Pract Oncol 5:634–644
7. Shweiki D, Itin A, Soffer D, Keshet E (1992) Vascular endothelial growth factor induced by hypoxia may mediate hypoxia-initiated angiogenesis. Nature 359:843–845
8. Rubenstein JL, Kim J, Ozawa T, Zhang M, Westphal M, Deen DF, Shuman MA (2000) Anti-VEGF antibody treatment of glioblastoma prolongs survival but results in increased vascular cooption. Neoplasia 2:306–314
9. Jain R, Scarpace L, Ellika S, Schultz L, Torcuator R, Hearshen D, Mikkelsen T Imaging response criteria for recurrent gliomas treated with bevacizumab: Role of diffusion weighted imaging as an imaging biomarker. J Neurooncol (in press)
10. Fischer I, Cunliffe CH, Bollo RJ, Raza S, Monoky D, Chiriboga L, Parker EC, Golfinos JG, Kelly PJ, Knopp EA, Gruber ML, Zagzag D, Narayana A (2008) High-grade glioma before and after treatment with radiation and Avastin: initial observations. Neuro Oncol 10:700–708
11. Kumar AJ, Leeds NE, Fuller GN, Van Tassel P, Maor MH, Sawaya RE, Levin VA (2000) Malignant gliomas: MR imaging spectrum of radiation therapy- and chemotherapy-induced necrosis of the brain after treatment. Radiology 217:377–384
12. Mullins ME, Barest GD, Schaefer PW, Hochberg FH, Gonzalez RG, Lev MH (2005) Radiation necrosis versus glioma recurrence: conventional MR imaging clues to diagnosis. AJNR Am J Neuroradiol 26:1967–1972
13. Rogers LR, Scarpace L, Guitterez J, Lord B, Ryu S, Movsas B, Honsowetz J, Rosenblum M, Jain R (2006) Magnetic resonance imaging characteristics and histological correlates of cerebral radiation necrosis. Neurology 66(Suppl 2):335
14. Zuniga RM, Torcuator R, Jain R, Anderson J, Doyle T, Ellika S, Schultz L, Mikkelsen T (2009) Efficacy, safety and patterns of response and recurrence in patients with recurrent high-grade gliomas treated with bevacizumab plus irinotecan. J Neurooncol 91:329–336
15. Henson JW, Ulmer S, Harris GJ (2008) Brain tumor imaging in clinical trials. AJNR Am J Neuroradiol 29:419–424
16. Jain RK, Tong RT, Munn LL (2007) Effect of vascular normalization by antiangiogenic therapy on interstitial hypertension, peritumor edema, and lymphatic metastasis: insights from a mathematical model. Cancer Res 67:2729–2735
17. Chong VF, Rumpel H, Fan YF, Mukherji SK (2001) Temporal lobe changes following radiation therapy: imaging and proton MR spectroscopic findings. Eur Radiol 11:317–324
18. Hein PA, Eskey CJ, Dunn JF, Hug EB (2004) Diffusion-weighted imaging in the follow-up of treated high-grade gliomas: tumor recurrence versus radiation injury. AJNR Am J Neuroradiol 25:201–209
19. Inoue T, Ogasawara K, Beppu T, Ogawa A, Kabasawa H (2005) Diffusion tensor imaging for preoperative evaluation of tumor grade in gliomas. Clin Neurol Neurosurg 107:174–180
20. Meyer MA, Frey KA, Schwaiger M (1993) Discordance between F-18 fluorodeoxyglucose uptake and contrast enhancement in a brain abscess. Clin Nucl Med 18:682–684
21. Law M, Young RJ, Babb JS, Peccerelli N, Chheang S, Gruber ML, Miller DC, Golfinos JG, Zagzag D, Johnson G (2008) Gliomas: predicting time to progression or survival with cerebral blood volume measurements at dynamic susceptibility-weighted contrast-enhanced perfusion MR imaging. Radiology 247:490–498
22. Law M, Yang S, Babb JS, Knopp EA, Golfinos JG, Zagzag D, Johnson G (2004) Comparison of cerebral blood volume and vascular permeability from dynamic susceptibility contrast-enhanced perfusion MR imaging with glioma grade. AJNR Am J Neuroradiol 25:746–755
23. Law M, Oh S, Babb JS, Wang E, Inglese M, Zagzag D, Knopp EA, Johnson G (2006) Low-grade gliomas: dynamic susceptibility-weighted contrast-enhanced perfusion MR imaging—prediction of patient clinical response. Radiology 238:658–667
24. Jain R, Ellika SK, Scarpace L, Schultz LR, Rock JP, Gutierrez J, Patel SC, Ewing J, Mikkelsen T (2008) Quantitative estimation of permeability surface-area product in astroglial brain tumors using perfusion CT and correlation with histopathologic grade. AJNR Am J Neuroradiol 29:694–700
25. Plate KH, Breier G, Weich HA, Risau W (1992) Vascular endothelial growth factor is a potential tumour angiogenesis factor in human gliomas in vivo. Nature 359:845–848
26. Jain RK (2002) Tumor angiogenesis and accessibility: role of vascular endothelial growth factor. Semin Oncol 29:3–9
27. Ellika SK, Jain R, Patel SC, Scarpace L, Schultz LR, Rock JP, Mikkelsen T (2007) Role of perfusion CT in glioma grading and comparison with conventional MR imaging features. AJNR Am J Neuroradiol 28:1981–1987
28. Covarrubias DJ, Rosen BR, Lev MH (2004) Dynamic magnetic resonance perfusion imaging of brain tumors. Oncologist 9:528–537
29. Barajas RF, Chang JS, Sneed PK, Segal MR, McDermott MW, Cha S (2009) Distinguishing recurrent intra-axial metastatic

tumor from radiation necrosis following gamma knife radiosurgery using dynamic susceptibility-weighted contrast-enhanced perfusion MR imaging. AJNR Am J Neuroradiol 30:367–372

30. Sugahara T, Korogi Y, Tomiguchi S, Shigematsu Y, Ikushima I, Kira T, Liang L, Ushio Y, Takahashi M (2000) Posttherapeutic intraaxial brain tumor: the value of perfusion-sensitive contrast-enhanced MR imaging for differentiating tumor recurrence from nonneoplastic contrast-enhancing tissue. AJNR Am J Neuroradiol 21:901–909

31. Jain R, Scarpace L, Ellika S, Schultz LR, Rock JP, Rosenblum ML, Patel SC, Lee TY, Mikkelsen T (2007) First-pass perfusion computed tomography: initial experience in differentiating recurrent brain tumors from radiation effects and radiation necrosis. Neurosurgery 61:778–786 Discussion 786–777

32. Gaensler EH, Dillon WP, Edwards MS, Larson DA, Rosenau W, Wilson CB (1994) Radiation-induced telangiectasia in the brain simulates cryptic vascular malformations at MR imaging. Radiology 193:629–636

33. Jain RK (2001) Normalizing tumor vasculature with anti-angiogenic therapy: a new paradigm for combination therapy. Nat Med 7:987–989

34. Kamiryo T, Lopes MB, Kassell NF, Steiner L, Lee KS (2001) Radiosurgery-induced microvascular alterations precede necrosis of the brain neuropil. Neurosurgery 49:409–414 Discussion 414–405

35. Chong VF, Rumpel H, Aw YS, Ho GL, Fan YF, Chua EJ (1999) Temporal lobe necrosis following radiation therapy for nasopharyngeal carcinoma: 1H MR spectroscopic findings. Int J Radiat Oncol Biol Phys 45:699–705

36. Weybright P, Sundgren PC, Maly P, Hassan DG, Nan B, Rohrer S, Junck L (2005) Differentiation between brain tumor recurrence and radiation injury using MR spectroscopy. AJR Am J Roentgenol 185:1471–1476

37. Smith EA, Carlos RC, Junck LR, Tsien CI, Elias A, Sundgren PC (2009) Developing a clinical decision model: MR spectroscopy to differentiate between recurrent tumor and radiation change in patients with new contrast-enhancing lesions. Am J Roentgenol 192:W45–W52

38. Rock JP, Scarpace L, Hearshen D, Gutierrez J, Fisher JL, Rosenblum M, Mikkelsen T (2004) Associations among magnetic resonance spectroscopy, apparent diffusion coefficients, and image-guided histopathology with special attention to radiation necrosis. Neurosurgery 54:1111–1117 Discussion 1117–1119

39. Sundgren PC (2009) MR spectroscopy in radiation injury. AJNR Am J Neuroradiol 30:1469–1476

40. Rabinov JD, Lee PL, Barker FG, Louis DN, Harsh GR, Cosgrove GR, Chiocca EA, Thornton AF, Loeffler JS, Henson JW, Gonzalez RG (2002) In vivo 3-T MR spectroscopy in the distinction of recurrent glioma versus radiation effects: initial experience. Radiology 225:871–879

41. Schlemmer HP, Bachert P, Henze M, Buslei R, Herfarth KK, Debus J, van Kaick G (2002) Differentiation of radiation necrosis from tumor progression using proton magnetic resonance spectroscopy. Neuroradiology 44:216–222

42. Schlemmer HP, Bachert P, Herfarth KK, Zuna I, Debus J, van Kaick G (2001) Proton MR spectroscopic evaluation of suspicious brain lesions after stereotactic radiotherapy. AJNR Am J Neuroradiol 22:1316–1324

43. Esteve F, Rubin C, Grand S, Kolodie H, Le Bas JF (1998) Transient metabolic changes observed with proton MR spectroscopy in normal human brain after radiation therapy. Int J Radiat Oncol Biol Phys 40:279–286

44. Kaminaga T, Shirai K (2005) Radiation-induced brain metabolic changes in the acute and early delayed phase detected with quantitative proton magnetic resonance spectroscopy. J Comput Assist Tomogr 29:293–297

45. Castillo M, Kwock L, Mukherji SK (1996) Clinical applications of proton MR spectroscopy. AJNR Am J Neuroradiol 17:1–15

46. Tien RD, Felsberg GJ, Friedman H, Brown M, MacFall J (1994) MR imaging of high-grade cerebral gliomas: value of diffusion-weighted echoplanar pulse sequences. AJR Am J Roentgenol 162:671–677

47. Sugahara T, Korogi Y, Kochi M, Ikushima I, Shigematu Y, Hirai T, Okuda T, Liang L, Ge Y, Komohara Y, Ushio Y, Takahashi M (1999) Usefulness of diffusion-weighted MRI with echo-planar technique in the evaluation of cellularity in gliomas. J Magn Reson Imaging 9:53–60

48. Gupta RK, Sinha U, Cloughesy TF, Alger JR (1999) Inverse correlation between choline magnetic resonance spectroscopy signal intensity and the apparent diffusion coefficient in human glioma. Magn Reson Med 41:2–7

49. Castillo M, Smith JK, Kwock L, Wilber K (2001) Apparent diffusion coefficients in the evaluation of high-grade cerebral gliomas. AJNR Am J Neuroradiol 22:60–64

50. Guo AC, Cummings TJ, Dash RC, Provenzale JM (2002) Lymphomas and high-grade astrocytomas: comparison of water diffusibility and histologic characteristics. Radiology 224:177–183

51. Chenevert TL, Stegman LD, Taylor JM, Robertson PL, Greenberg HS, Rehemtulla A, Ross BD (2000) Diffusion magnetic resonance imaging: an early surrogate marker of therapeutic efficacy in brain tumors. J Natl Cancer Inst 92:2029–2036

52. Hamstra DA, Galban CJ, Meyer CR, Johnson TD, Sundgren PC, Tsien C, Lawrence TS, Junck L, Ross DJ, Rehemtulla A, Ross BD, Chenevert TL (2008) Functional diffusion map as an early imaging biomarker for high-grade glioma: correlation with conventional radiologic response and overall survival. J Clin Oncol 26:3387–3394

53. Field AS, Alexander AL, Wu YC, Hasan KM, Witwer B, Badie B (2004) Diffusion tensor eigenvector directional color imaging patterns in the evaluation of cerebral white matter tracts altered by tumor. J Magn Reson Imaging 20:555–562

54. Morita K, Matsuzawa H, Fujii Y, Tanaka R, Kwee IL, Nakada T (2005) Diffusion tensor analysis of peritumoral edema using lambda chart analysis indicative of the heterogeneity of the microstructure within edema. J Neurosurg 102:336–341

55. Basser PJ, Pierpaoli C (1996) Microstructural and physiological features of tissues elucidated by quantitative-diffusion-tensor MRI. J Magn Reson B 111:209–219

56. Wiegell MR, Henson JW, Tuch DS, Sorensen AG: Diffusion tensor imaging shows potential to differentiate infiltrating from non-infiltrating tumors. In: Proceedings of the international society for magnetic resonance in medicine (ISMRM) eleventh scientific meeting, Toronto, Ontario, Canada, p 2075

57. Sundgren PC, Fan X, Weybright P, Welsh RC, Carlos RC, Petrou M, McKeever PE, Chenevert TL (2006) Differentiation of recurrent brain tumor versus radiation injury using diffusion tensor imaging in patients with new contrast-enhancing lesions. Magn Reson Imaging 24:1131–1142

58. Le Bihan D, Douek P, Argyropoulou M, Turner R, Patronas N, Fulham M (1993) Diffusion and perfusion magnetic resonance imaging in brain tumors. Top Magn Reson Imaging 5:25–31

59. Tung GA, Evangelista P, Rogg JM, Duncan JA 3rd (2001) Diffusion-weighted MR imaging of rim-enhancing brain masses: is markedly decreased water diffusion specific for brain abscess? AJR Am J Roentgenol 177:709–712

60. Biousse V, Newman NJ, Hunter SB, Hudgins PA (2003) Diffusion weighted imaging in radiation necrosis. J Neurol Neurosurg Psychiatry 74:382–384

61. Zhou XJ, Leeds NE, Kumar AJ, Chong J, Levin VA: Differentiation of tumor recurrence from treatment-induced necrosis using quantitative diffusion MRI. In: Proceedings, ninth scientific

meeting, international society of magnetic resonance in medicine, Glasgow, Scotland, UK, p 726

62. Asao C, Korogi Y, Kitajima M, Hirai T, Baba Y, Makino K, Kochi M, Morishita S, Yamashita Y (2005) Diffusion-weighted imaging of radiation-induced brain injury for differentiation from tumor recurrence. AJNR Am J Neuroradiol 26:1455–1460

63. Sinha S, Bastin ME, Whittle IR, Wardlaw JM (2002) Diffusion tensor MR imaging of high-grade cerebral gliomas. AJNR Am J Neuroradiol 23:520–527

64. Nagesh V, Tsien CI, Chenevert TL, Ross BD, Lawrence TS, Junick L, Cao Y (2008) Radiation-induced changes in normal-appearing white matter in patients with cerebral tumors: a diffusion tensor imaging study. Int J Radiat Oncol Biol Phys 70:1002–1010

65. Kashimura H, Inoue T, Beppu T, Ogasawara K, Ogawa A (2007) Diffusion tensor imaging for differentiation of recurrent brain tumor and radiation necrosis after radiotherapy—three case reports. Clin Neurol Neurosurg 109:106–110

66. Chao ST, Suh JH, Raja S, Lee SY, Barnett G (2001) The sensitivity and specificity of FDG PET in distinguishing recurrent brain tumor from radionecrosis in patients treated with stereotactic radiosurgery. Int J Cancer 96:191–197

67. Stokkel M, Stevens H, Taphoorn M, Van Rijk P (1999) Differentiation between recurrent brain tumour and post-radiation necrosis: the value of 201Tl SPET versus 18F-FDG PET using a dual-headed coincidence camera—a pilot study. Nucl Med Commun 20:411–417

68. Tsuyuguchi N, Sunada I, Iwai Y, Yamanaka K, Tanaka K, Takami T, Otsuka Y, Sakamoto S, Ohata K, Goto T, Hara M (2003) Methionine positron emission tomography of recurrent metastatic brain tumor and radiation necrosis after stereotactic radiosurgery: is a differential diagnosis possible? J Neurosurg 98:1056–1064

69. Patronas NJ, Di Chiro G, Brooks RA, DeLaPaz RL, Kornblith PL, Smith BH, Rizzoli HV, Kessler RM, Manning RG, Channing M, Wolf AP, O'Connor CM (1982) Work in progress: [18F] fluorodeoxyglucose and positron emission tomography in the evaluation of radiation necrosis of the brain. Radiology 144:885–889

70. Kim CK, Alavi JB, Alavi A, Reivich M (1991) New grading system of cerebral gliomas using positron emission tomography with F-18 fluorodeoxyglucose. J Neurooncol 10:85–91

71. De Witte O, Goldberg I, Wikler D, Rorive S, Damhaut P, Monclus M, Salmon I, Brotchi J, Goldman S (2001) Positron emission tomography with injection of methionine as a prognostic factor in glioma. J Neurosurg 95:746–750

72. Choi SJ, Kim JS, Kim JH, Oh SJ, Lee JG, Kim CJ, Ra YS, Yeo JS, Ryu JS, Moon DH (2005) [18F]3′-deoxy-3′-fluorothymidine PET for the diagnosis and grading of brain tumors. Eur J Nucl Med Mol Imaging 32:653–659

73. Spence AM, Muzi M, Link JM, O'Sullivan F, Eary JF, Hoffman JM, Shankar LK, Krohn KA (2009) NCI-sponsored trial for the evaluation of safety and preliminary efficacy of 3′-deoxy-3′-[18F]fluorothymidine (FLT) as a marker of proliferation in patients with recurrent gliomas: preliminary efficacy studies. Mol Imaging Biol 11:343–355

74. Chen W, Silverman DH, Delaloye S, Czernin J, Kamdar N, Pope W, Satyamurthy N, Schiepers C, Cloughesy T (2006) 18F-FDOPA PET imaging of brain tumors: comparison study with 18F-FDG PET and evaluation of diagnostic accuracy. J Nucl Med 47:904–911

75. Huisman TA, Loenneker T, Barta G, Bellemann ME, Hennig J, Fischer JE, Il'yasov KA (2006) Quantitative diffusion tensor MR imaging of the brain: field strength related variance of apparent diffusion coefficient (ADC) and fractional anisotropy (FA) scalars. Eur Radiol 16:1651–1658

76. Sorensen AG, Batchelor TT, Zhang WT, Chen PJ, Yeo P, Wang M, Jennings D, Wen PY, Lahdenranta J, Ancukiewicz M, di Tomaso E, Duda DG, Jain RK (2009) A "vascular normalization index" as potential mechanistic biomarker to predict survival after a single dose of cediranib in recurrent glioblastoma patients. Cancer Res 69:5296–5300

77. Galban CJ, Chenevert TL, Meyer CR, Tsien C, Lawrence TS, Hamstra DA, Junck L, Sundgren PC, Johnson TD, Ross DJ, Rehemtulla A, Ross BD (2009) The parametric response map is an imaging biomarker for early cancer treatment outcome. Nat Med 15:572–576

78. Pope WB, Kim HJ, Huo J, Alger J, Brown MS, Gjertson D, Sai V, Young JR, Tekchandani L, Cloughesy T, Mischel PS, Lai A, Nghiemphu P, Rahmanuddin S, Goldin J (2009) Recurrent glioblastoma multiforme: ADC histogram analysis predicts response to bevacizumab treatment. Radiology 252:182–189

79. Moffat BA, Chenevert TL, Meyer CR, McKeever PE, Hall DE, Hoff BA, Johnson TD, Rehemtulla A, Ross BD (2006) The functional diffusion map: an imaging biomarker for the early prediction of cancer treatment outcome. Neoplasia 8:259–267